DOI: 10.1002/ejic.201001357

Intermolecular Hydrogen–Fluorine Interaction in Dimolybdenum Triply Bonded Complexes Modified by Fluorinated Formamidine Ligands for the Construction of 2D- and 3D-Networks

Sebastian Krackl,[a,b] Shigeyoshi Inoue,[b] Matthias Driess,[a,b] and Stephan Enthaler*[a]

Keywords: Molybdenum / Fluorine / Fluorinated ligands / N ligands / Heteroleptic complexes / Multiple bonds / Crystal engineering / Hydrogen-fluorine interactions

The formamidines ArNHC(H)=N–Ar [Ar = Ph (**2a**), 4-F-Ph (**2b**), 3,5-F_2Ph (**2c**) and 2,6-F_2Ph (**2d**) and R = 2,3,5-F_3Ph (**2e**), 3,4,5-F_3Ph (**2f**), F_5Ph (**2g**) and 4-CF_3Ph (**2h**)] were synthesized and the influence of the introduction of a fluorine or a trifluoromethyl group into the aryl unit on the solid-state structures was investigated. On comparing the experimental data, only marginal differences in the geometrical and electronic features of the diverse substituted species were detected. DFT calculations and X-ray crystallography of **2d**–**2g** revealed that the *E*-*syn*-configuration corresponded to the thermodynamically most stable motif of all of the examined formamidines. However, in their solid-state, these ligands showed a range of H···F interactions, which varied depending on the number and position of the fluorine atoms on the aryl group and thus led to interesting solid-state structures. Moreover, compounds **2** were used for the synthesis of the new heteroleptic dimolybdenum triply-bonded complexes, Mo_2[(**2a**–**2c**; **2e**–**f**)–H]$_2$(O*t*Bu)$_4$ (**3a**–**3c**; **3e**–**3f**). X-ray crystallography of complexes **3c** and **3f** revealed two different isomers in the solid state: in *trans*-**3c** the two formamidines are in one plane, while in *cis*-**3c** and *cis*-**3f** they are next to each other. The DFT calculations showed only a small distinction in energy between the configurations, which led us to assume that the different configurations were induced by the crystal packing. The specific H···F interactions provided by the different formamidines led to a two-dimensional arrangement for *trans*-**3c** and a three-dimensional network for *cis*-**3c** and *cis*-**3f**.

Introduction

The replacement of hydrogen by the sterically similar fluorine atom in organic molecules has a tremendous effect on the properties of the obtained material.[1] This is demonstrated by the extensive range of applications of these materials, for example, bulk chemicals, pharmaceuticals, agrochemicals, polymers, solvents and as key intermediates in organic syntheses.[2] Furthermore, the exchange of carbon-bonded hydrogen with fluorine in the ligand scaffold in organometallic complexes usually leads to alterations in the physical and chemical properties of the respective compound. The high electronegativity and the low polarizability of the fluorine atom are the main reasons for the modifications. In addition, the influence of this substitution is observed in the study of the solid-state structures. Fluorine has the capacity to form various intermolecular interactions, especially phenyl-perfluorophenyl-, C–F···H, F···F, C–F···π_F and C–F···metal interactions, that significantly alter the intra- and intermolecular interactions in the crystal.[1,3,4] During the last decades complexes have been reported that cover several types of fluorine interactions.[5–7] For example, Cotton et al. reported on the coordination of fluorinated *N*,*N*′-bis(phenyl)formamidines ligands to chromium.[8,9] The obtained complexes consist of the structural motif Cr_2L_4, which means that the four formamidine ligands are bonded to the quadruply bonded metal centre. The structural information showed a Cr···F interaction for the *ortho*-fluorine on the phenyl ring of the ligand. So far, to the best of our knowledge, the equivalent metal–metal bonded systems for the higher homologues of chromium, namely molybdenum and tungsten, have not been synthesized. Thus, we were interested in studying the coordination of these types of ligands towards these metals. The coordination of non-fluorine substituted formamidine to quadruply-bonded molybdenum complexes has been demonstrated, while neutral, triply-bonded dimolybdenum analogues have not been reported as yet. Undoubtedly, triply-bonded molybdenum complexes are of interest because of their applicability as precursor for heterogeneous materials[10] and as precursor for heterobimetallic compounds,[11] which makes them profitable systems for further applications. Recently, some of us synthesized monodentate Mo≡Mo alkoxides,[11,12] which exhibit the general motif of

[a] Technische Universität Berlin, Department of Chemistry,Cluster of Excellence "Unifying Concepts in Catalysis", Straße des 17. Juni 135/C2, 10623 Berlin, Germany
Fax: +49-30314 29732
E-mail: stephan.enthaler@tu-berlin.de
[b] Institute of Chemistry: Metalorganics and Inorganic Materials, Technische Universität Berlin, Straße des 17. Juni 135, Sekr. C2, 10623 Berlin, Germany
Supporting information for this article is available on the WWW under http://dx.doi.org/10.1002/ejic.201001357.

an "ethane-like" structure with a staggered ligand conformation and unequally oriented ligands with different Mo···O distances at each of the molybdenum atoms.[13] Based on these types of complexes we were interested in the coordination abilities of the formamidine ligands. In this work, fluorinated formamidine ligands will be studied with regards to the fluorine interactions and the consequent formation of 2D- and 3D-networks in the crystal.

Results and Discussion

The formamidines **2** were synthesized by following the reported procedures. Two equivalents of the corresponding aniline were treated with triethyl orthoformate under refluxing conditions (Scheme 1). The crude products were purified by recrystallization from *n*-hexane to obtain **2** in fair to good yields. Notably, in all of the cases the *E*-isomer selectively formed, which is in accordance with the literature.[14]

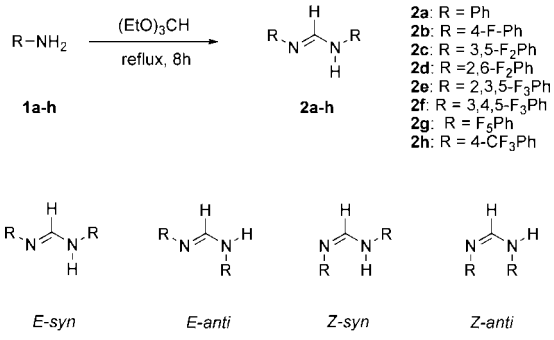

Scheme 1. The synthesis of the substituted *N*,*N*′-bis(phenyl)formamidines (**2**).

In addition, we studied the influence of the various substituents in comparison to the parent structure **2a**, and in particular the effect of the fluorine substitution. The typical analytical parameters are given in Table 1. In order to detect geometrical and electronic changes, the formamidine proton was applied as a sensor. A significant influence on the ^{1}H NMR chemical shift was found when the number of fluoro substituents on the aryl unit was increased, however, no effect was observed when a *para*-trifluoromethyl group was embedded. In general, only a marginal influence was seen when the formamidine carbon was used as the sensor, since all of the ^{13}C NMR spectroscopic values are in the range of 149 to 151 ppm. However, a significant shift of 159.0 ppm was measured for ligand **2h**.

In order to get insight into the geometrical structure of the formamidines (Scheme 2), DFT-calculations at the RB3LYP/6-31++G(d,p) level were performed. The *E-syn*-configuration corresponded to the most thermodynamically stable motif (Table 2), which is in agreement with the experimental observations. This was further confirmed by single-crystal X-ray crystallography, since in all of the cases the *E-syn*-isomer was obtained.

In addition, a different orientation of the aryl groups was observed in the molecular structures for the compounds **2d**, **2e** and **2g**, all of which exhibit a fluorine atom in the *ortho*-position. The aryl groups in these compounds were symmetrically oriented to each other (see Figure 1).

Table 1. Characterization of formamidines **2**.

L	^{1}H NMR [ppm][a]	^{13}C NMR [ppm][b]	IR [cm^{-1}][c]	λ [cm^{-1}][d]
2a	8.24	149.5	1679	281.5
2b	8.07	150.2	1671	279.5
2c	8.03	149.1	1676	294.5
2d	7.94	154.3	1669	268.0
2e	8.14	149.8	1672	292.0
2f	7.89	150.2	1677	271.0
2g	8.28	–	1678	264.5
2h	8.21	159.0	1672	300.8

[a] The chemical shift (^{1}H NMR) for RN=C(*H*)NHR was measured in [D$_1$]chloroform at 25 °C. [b] The chemical shift (^{13}C NMR) for RN=*C*(H)NHR was measured in [D$_1$]chloroform at 25 °C. [c] KBr. [d] All of the measurements were carried out in CH_3CN at 25 °C.

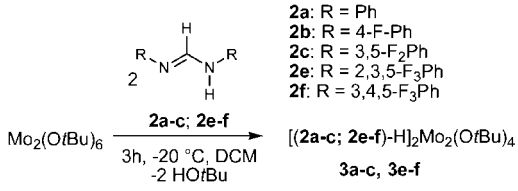

Scheme 2. The synthesis of the complexes Mo_2[(**2a**–**2c; 2e**–**2f**)–H]$_2$(O*t*Bu)$_4$ (**3a**–**3c; 3e**–**3f**).

Table 2. The calculated and observed geometrical details for **2**.

	2a	**2b**	**2c**	**2d**	**2e**	**2f**	**2g**	**2h**
N1–C1 [Å]	1.284	1.283	1.283	1.284	1.283	1.283	1.285	1.283
Observed	–	1.283[a]	–	1.286	1.298	1.280	1.311	–
N2–C1 [Å]	1.369	1.369	1.369	1.371	1.375	1.369	1.374	1.369
Observed	–	1.342[a]	–	1.344	1.331	1.351	1.331	–
N1–C1–N2 [°]	119.8	119.8	119.5	118.3	117.8	119.5	118.0	120.5
Observed	–	122.6[a]	–	120.5	122.2	121.8	121.0	–

[a] The values for **2b** were taken from ref.[14]

Short intramolecular Ar–F···H–C(=NAr)NHAr distances for compounds **2d**, **2e** and **2g** were observed (2.356–2.502 Å), which most probably favours this geometry since for **2f** the aryl groups are twisted towards each other at an angle of nearly 90°. In their solid-state, these compounds show a variety of dimensional networks that were mediated by the H···F interactions, which include the short Ar–F···H$_{para}$–Ar, Ar–F···H–C(=NAr)NHAr and Ar–F···F–Ar distances as well as the stacking interactions between the adjacent aryl units (for a detailed description, see Supporting Information).

At this point we were interested in attaching the studied formamidines to transition metals in order to design metal-containing dimensional networks. We decided to coordinate the fluorine substituted formamidines to the dimolybdenum triple bond by means of a direct protolysis reaction of **2** with Mo_2(O*t*Bu)$_6$.[15] The starting material Mo_2(O*t*Bu)$_6$ was easily accessible by means of salt metathesis from Mo_2Cl_6(dme)$_2$[16] (dme = dimethoxyethane). A ratio of 2:1 [ligand: Mo_2(O*t*Bu)$_6$] was chosen, which should theoretic-

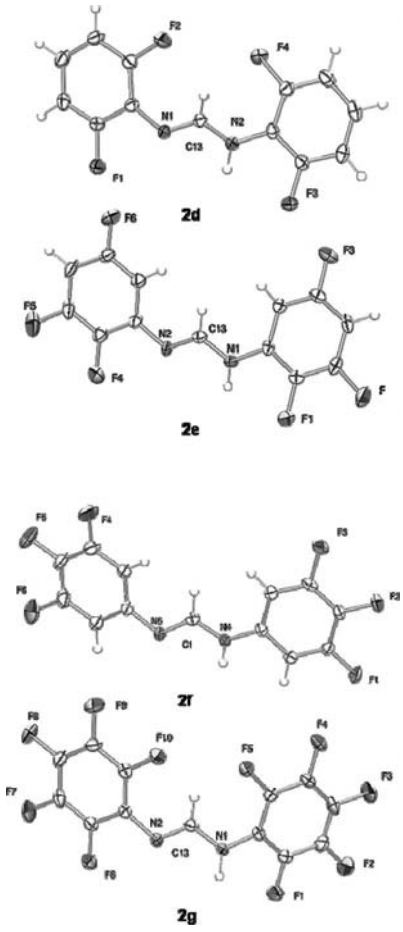

Figure 1. The molecular structures for **2d**–**2g**. The thermal ellipsoids are drawn at the 50% probability level. The solvent molecules for **2g** (toluene) are omitted for clarity.

ally lead to a partial substitution of the alkoxy ligands, in order to investigate the coordination preference of the dimolybdenum centre and to retain the solubility of the complexes in nonpolar solvents. The addition of **2a**–**2c** and **2e**–**2f** to $Mo_2(OtBu)_6$ resulted in a partial protolysis and afforded the complexes Mo_2[(**2a**–**2c**; **2e**–**2f**)–H]$_2(OtBu)_4$ (**3a**–**3c**; **3e**–**3f**) (Scheme 2). To the best of our knowledge, **3** are the first neutral, triply-bonded dimolybdenum complexes that bear a formamidine ligand.

The complexes formed by the reaction of formamidines **2d** and **2g** with $Mo_2(OtBu)_6$ could not be obtained in an analytically pure form (mismatching elemental analysis), although the ^{1}H NMR spectra appeared to be fairly clean, and thus these complexes are not discussed. Furthermore, the reaction of **2h** with $Mo_2(OtBu)_6$ led to a complex mixture of products that did not include the desired triply–bonded complex. Changing the reaction conditions has not resulted in a suitable outcome for this reaction as yet. The complexes **3a**–**3c** and **3e**–**3f** are green–brown powders that are extraordinarily sensitive towards oxygen and moisture. They decomposed without subliming between 80 and 100 °C and did not give rise to the appropriate mass spectra. In the ^{1}H NMR spectra successful coordination was easily followed by the disappearance of the N–H proton signal. The peaks that correspond to the proton at the carbon atom in the formamidine functionality are significantly shifted to the lower field as compared to those of the non-shifted signal for the uncoordinated species (Table 3).

Table 3. Selected NMR data (δ values, ppm)[a] for **3a**–**3c** and **3e**–**3f**.

L	–N=*C*(*H*)N–^{1}H NMR	^{13}C NMR	–OC(*CH*$_3$)$_3$^{1}H NMR	^{13}C NMR	–Ar$H_{5-n}F_n$^{1}H NMR
3a	8.83	169.6	1.32	33.0	6.13–6.32
3b	8.88	176.3	1.40	32.2	6.11–6.32
3c	8.97	176.0	1.43	32.1	6.00–6.28
3e	9.13	179.1	1.44	32.8	6.07–6.36
3f	8.87	175.9	1.46	32.3	6.13–6.29

[a] The chemical shifts (^{1}H and ^{13}C NMR spectroscopy) were measured in [D_1]chloroform at 25 °C.

In contrast, the signal corresponding to the *tert*-butoxy protons shifted to a higher field compared to that of the homoleptic analogue, $Mo_2(OtBu)_6$. This phenomenon has been observed in other heteroleptic complexes[17] and is probably caused by the change in orientation of the O*t*Bu groups, which consequently results in a different magnetic environment due to the magnetic anisotropy of the dimolybdenum triple bond.[11] The strong shift to a lower field of the methine proton (N=C*H*–N) can also be attributed to the diamagnetic anisotropy, since it is placed over the centre of the triple bond and thus strongly deshielded.[12] In both the ^{1}H NMR and the ^{13}C NMR spectra we observed only one set of broad signals for both of the aryl ligands on the same formamidine. This implied a symmetrical bonding contribution for both of the nitrogen atoms. The assumed ligand distribution in the complexes was confirmed by the matching integral ratios for the corresponding proton signals. Since solvent molecules are readily lost from the recrystallized material, it was crushed and dried in vacuo at elevated temperatures and, thus, no residual signals for the solvent molecules (neither toluene nor dichloromethane) were observed in the spectra.

Further evidence was provided by the single-crystal X-ray diffraction data. Suitable single crystals for compounds **3c** and **3f** were obtained from toluene/dichloromethane (DCM). Compound **3c** crystallizes in the monoclinic space group, $P2_1/c$ with Z = 2, and one cocrystallized toluene molecule was found in the unit cell (Figure 2).

The Mo–Mo distance for *trans*-**3c**·toluene (2.253 Å) is slightly elongated compared to that of other Mo≡Mo complexes. This is probably due to the substitution with a bridging ligand that enforces the eclipsed conformation as reported for other compounds (Table 4).[15] The Mo–N bond distances are statistically identical with 2.175 and 2.183 Å and are in the expected range. Each formamidine constitutes a planar five-membered ring with the molybdenum atoms. The Mo–Mo–N1 and Mo–Mo–N2 bond angles of 90.69 and 91.01°, respectively, are close to each other and both formamidine ligands are opposite to each other in one plane.

The Mo–O bond distances are 1.901 and 1.931 Å for both of the molybdenum atoms and the alkoxide ligands

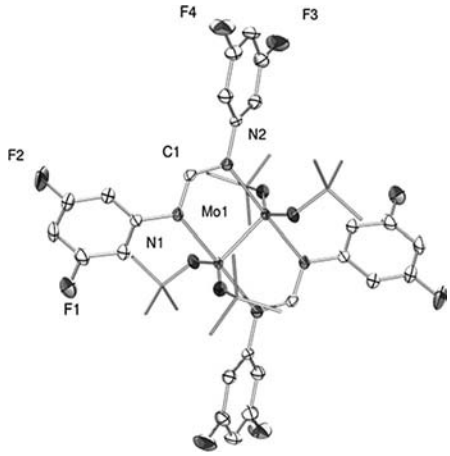

Figure 2. The ORTEP presentation of complex *trans*-**3c**. The hydrogen atoms and the solvent molecules (toluene) are omitted for clarity.

Table 4. Selected bond lengths [Å] and angles [°] for *trans*-**3c**, *cis*-**3c** and *cis*-**3f**.

	trans-**3c**·toluene[a]	*cis*-**3c**·cyclopentane	*cis*-**3f**·DCM
Mo1–Mo2	2.253(4)	2.2503(5)	2.256(1)
Mo1–N1	2.175(3)	2.176(4)	2.174(6)
Mo1–N3	2.175(3)	2.221(4)	2.247(7)
Mo2–N2	2.183(3)	2.232(4)	2.243(6)
Mo2–N4	2.183(3)	2.194(4)	2.176(7)
Mo1–O1	1.901(3)	1.912(3)	1.896(5)
Mo1–O2	1.931(2)	1.891(3)	1.899(5)
Mo2–O3	1.901(3)	1.883(4)	1.864(6)
Mo2–O4	1.931(2)	1.908(3)	1.910(5)
Mo1–Mo2–O1	112.2(7)	101.3(1)	110.3(2)
Mo1–Mo2–O2	101.1(7)	110.8(1)	101.3(2)
Mo1–Mo2–O3	112.2(7)	110.9(1)	112.0(2)
Mo1–Mo2–O4	101.1(7)	100.6(1)	102.2(2)
Mo1–Mo2–N1	90.6(8)	92.5(1)	92.8(2)
Mo1–Mo2–N2	91.0(8)	87.6(1)	88.1(2)
Mo1–Mo2–N3	90.6(8)	87.6(1)	87.8(2)
Mo1–Mo2–N4	91.0(8)	92.6(1)	93.0(2)
N1–Mo1–O1	90.1(1)	150.2(1)	151.3(2)

[a] For *trans*-**3c** Mo2=Mo1′, O1=O3, O2=O4, N1=N3, N2=N4.

are oriented differently in space: one points towards the Mo–Mo triple bond and the other one points away from the Mo–Mo triple bond.

In contrast, we obtained a different structural motif from the crystallization of compound *cis*-**3f** under similar conditions. Compound **3f** crystallizes in the triclinic space group, $P\bar{1}$, with $Z = 2$. The Mo–Mo distances for *trans*-**3c** and *cis*-**3f** are in a similar range, with a bond length of 2.256 Å for the latter (Figure 3). However, in the molecular structure of complex *cis*-**3f** no planar ring between the formamidine and the triple bond is constituted and the Mo–N bond distances for the same ligand differ strongly (average 2.174 and 2.245 Å), which indicates a weaker Lewis base donation of the ligand nonbonding nitrogen. The two O*t*Bu ligands attached to the same molybdenum atom also have a different orientation in space. Intriguingly, the Mo2–O bond distances differ from each other (1.864 and 1.910 Å), but the Mo1–O distances are statistically identical (1.896 and 1.899 Å). In order to understand the reason for the two different configurations observed for **3**, we decided to perform DFT calculations at the B3LYP level. For both compounds the calculations showed an almost equal stability for both confirmations, with a slightly higher stability for the *trans*-configuration, with 1.59 kcal mol^{-1} for **3c** and 1.29 kcal mol^{-1} for **3f**. Simulating the molecular orbitals for the *cis*-configuration did not reveal any delocalization of the electron density over the ligand or the triple bond in both cases. This means that, most probably, packing effects, and thus the specific H···F interactions formed by the respective ligand as well as the nature of the cocrystallized solvent, are responsible for the change in configuration, since we assumed fast ligand scrambling with the involvement of a rapid change from terminal to bridging modes for the alkoxy ligands in solution, as reported for other triply-bonded dimolybdenum complexes.[18] Further proof for this assumption was provided by the solvent exchange experiments. Therefore, we recrystallized complex **3c** in a 1:1 mixture of cyclopentane/DCM instead of the 1:1 mixture of toluene/DCM applied in the synthesis. After cooling to –20 °C for two weeks, we obtained crystals that significantly differed in their crystal morphology. The complementary structure of **3c**, namely, the *cis*-configuration, was observed by means of single-crystal X-ray diffraction measurements (Figure 4) and cyclopentane replaced the cocrystallized toluene.

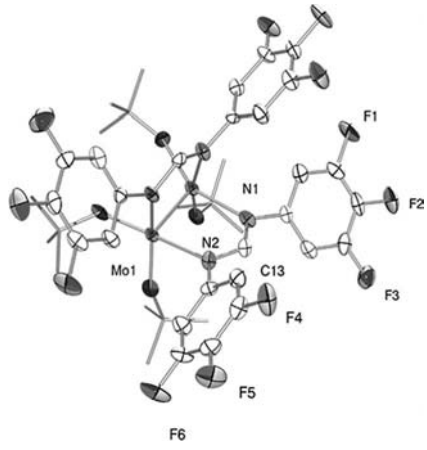

Figure 3. The ORTEP presentation of complex *cis*-**3f**. The hydrogen atoms, the solvent molecules (DCM) and the equal ligands are omitted for clarity.

The *cis*-isomers of **3f** and **3c** show very similar structural features, namely, similar Mo–Mo, Mo–N and Mo–O bond lengths and the resulting bond angles, and thus only a small amount of change is induced in the molecule by varying the fluorine substitution pattern of the aryl ligand (Table 4). The latter results support the assumption that there is a rapid equilibrium between the *cis*/*trans*-configurations in solution and that the observed isomers in the solid state are determined by the crystal packing. However, more detailed experimental and theoretical investigations on this subject are in progress.

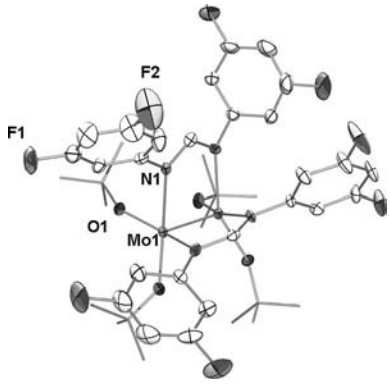

Figure 4. The ORTEP presentation of complex *cis*-**3c**. The hydrogen atoms, the solvent molecules (cyclopentane) and the equal ligands are omitted for clarity.

Further investigation into the solid-state structures of the obtained complexes showed that the formamidines are an excellent tool for the design of transition metal-containing dimensional networks that are mediated by H···F interactions. In the solid-state structure of *trans*-**3c**, short Ar–F···H–C(NAr)$_2$ interactions are present (2.403 Å) with a F···H–C bond angle of 153.99°, longer Ar–F···H–Ar interactions of 2.540 and 2.625 Å are also present with F···H–C bond angles of 132.48 and 121.81°, respectively (Figure 5).

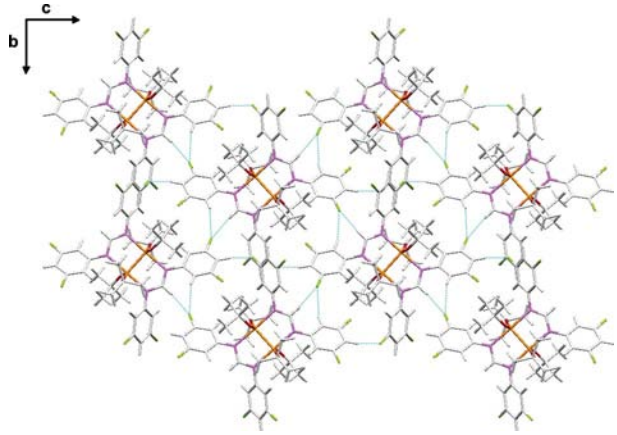

Figure 5. A cut-out along the bc-plane of the crystal structure for complex *trans*-**3c**. The solvent molecules (toluene) are omitted for clarity. The blue lines represent the Ar–F···H–C(NAr)$_2$ interactions (2.403 Å) and the F···H–C bond angle of 153.99°, as well as the longer Ar–F···H–Ar interactions (2.540 and 2.625 Å) with the F···H–C bond angles of 132.48 and 121.81°.

These F···H interactions led to a planar arrangement of the subunits in the bc plane without short contacts between the different planes. The O*t*Bu ligands are sited above and beneath these planes and are in separate, adjacent planes from each other. The cocrystallized toluene is found in the interspaces between the layers.

The solid-state structure of *cis*-**3f** varies strongly from the described network of *trans*-**3c** and shows a similar appearance to that of the noncoordinated ligand **2f** (see Supporting Information).

No short Ar–F···H–C(NAr)$_2$ contacts are present for *cis*-**3f**, as observed in the crystal structure of the free ligand **2f**. However, the H···F interactions are present between the Ar–fluorine atoms and the protons at the O*t*Bu groups (average 2.675 Å) and the stacking interactions are present between the adjacent molecules with an aryl···aryl average distance of 3.429 Å (Figure 6). These interactions result in the construction of a three-dimensional network. For the solid-state structure of *cis*-**3c** we obtained a similar picture as for *cis*-**3f**, namely, a three-dimensional network. However, in this case, no stacking interactions and only short H···F–Ar interactions were observed. Unfortunately, recrystallization of the synthesized complexes **3a**, **3b** and **3e** did not afford crystals that were suitable for single-crystal X-ray diffraction measurements, and thus, the potential Mo···F interactions could not be observed. Attempts concerning this matter are still in progress.

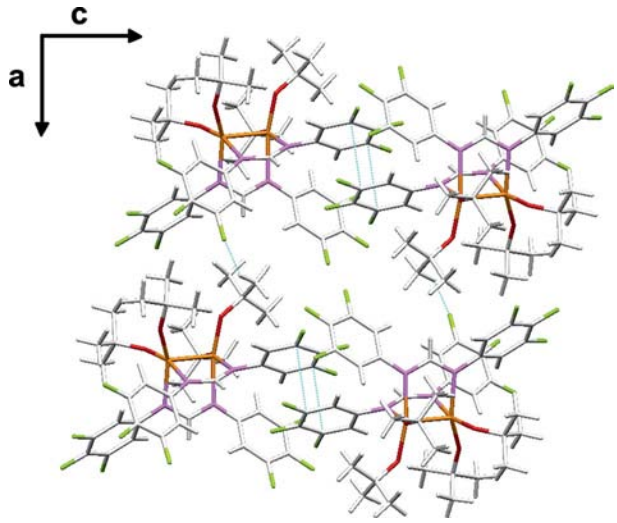

Figure 6. A cut-out along the ac plane of the crystal structure for complex *cis*-**3f**. The solvent molecules (DCM) are omitted for clarity. The blue lines represent the H···F contacts between the Ar–fluorine atoms and the protons at the O*t*Bu groups (average 2.675 Å) and the Ar–F···Ar–F distance (average 3.429 Å) between the parallel-stacked aryl substituents. The cocrystallized DCM molecules are accommodated in the voids of the network, which has a short Ar–F···H$_2$CCl$_2$ distance that is in the range of 2.575–2.655 Å.

Conclusions

In summary we have demonstrated the application and usefulness of fluorine-substituted formamidines for the construction of dimensional networks. Firstly the formamidines **2a**–**2h** were synthesized and investigated in detail concerning the effect of fluorine and trifluoromethyl substitution on the properties of the ligand and its influence on their corresponding solid-state structures. Although the experimental data only showed marginal differences in the geometrical and electronic features between the diverse substituted species, these compounds showed manifold H···F interactions, which specifically altered the solid-state structure of the corresponding compound and led to 2D- and

3D-networks with different appearances. Having synthesized these fluorinated formamidines, we questioned whether this specificity could be applied in order to design the solid-state structures of the corresponding metal complexes. The formamidine ligands were coordinated to a triply-bonded dimolybdenum complex and, depending on the position of the fluorine and the applied solvent, different crystal morphologies and different configurations for the resulting complexes, $Mo_2[(\mathbf{2a}–\mathbf{2c}; \mathbf{2e}–\mathbf{2f})–H]_2(O\mathit{t}Bu)_4$, were observed. For instance, *trans*-**3c** displayed a planar configuration for the attached formamidines and the molecular subunits constructed a 2D-arrangement by means of the H···F interactions, while in the corresponding *cis*-isomer (*cis*-**3c** or *cis*-**3f**) the ligands were oriented next to each other and the specific interactions lead to the formation of a three-dimensional network.

Experimental Section

General: All of the manipulations with oxygen- and moisture-sensitive compounds were performed under dinitrogen by using the standard Schlenk technique. ^1H, ^{19}F and ^{13}C NMR spectra were recorded with a Bruker AFM 200 spectrometer (^1H: 200.13 MHz; ^{13}C: 50.32 MHz; ^{19}F: 188.31 MHz) and by using the proton signals of the deuterated solvents as the reference. The single-crystal X-ray diffraction measurements were recorded with an Oxford Diffraction Xcalibur S Saphire spectrometer. The IR spectra were recorded either with a Nicolet Series II Magna-IR-System 750 FTR-IR instrument or with a Perkin–Elmer Spectrum 100 FTIR instrument. The electron ionisation mass spectra (EI-MS) were recorded with a Finnigan MAT95S instrument. The melting points (m.p.) were determined with a BSGT Apotec II capillary-tube apparatus and are uncorrected. The UV/Vis spectra were recorded with a Perkin–Elmer Lambda 20 spectrometer at ambient temperature. The elemental analyses were performed with a Perkin–Elmer Series II CHNS/O Analyzer 2400 instrument.

Single-Crystal X-ray Structure Determinations: The single crystals were mounted on a glass capillary in perfluorinated oil and measured in a cold steam of N_2. The data for **2d**–**2g**, *trans*-**3c**, *cis*-**3c** and *cis*-**3f** were collected with an Oxford Diffraction Xcalibur S Saphire at 150 K (Mo-K_α radiation, λ = 0.71073 Å, ω-scan). The structures were solved by direct methods. The refinements were carried out with the SHELXL-97 package.[19] All of the thermal displacement parameters were refined anistropically for non-hydrogen atoms and the positions of the hydrogen atoms were calculated and considered isotropically according to a riding model. All of the refinements were carried out by full-matrix least-squares refinement on F^2. The crystallographic data for the seven compounds are summarized in Table 5.

CCDC-793747 (for *trans*-**3c**), -793752 (for *cis*-**3f**) and -808037 (for *cis*-**3c**) contain the supplementary crystallographic data for this paper. These data can be obtained free of charge from The Cambridge Crystallographic Data Centre via www.ccdc.cam.ac.uk/data_request/cif.

General Synthesis of *N,N′*-Bis(phenyl)formamidines: A mixture of the corresponding aniline (50 mmol) and triethyl orthoformate (25 mmol) was heated under reflux for 12 h. All of the volatiles were removed in vacuo and the residue was washed with *n*-hexane to yield a white powder.

***N,N′*-Bisphenylformamidine (2a):**[20,21] Yield 76% (3.7 g); m.p. 139 °C (crystallized from *n*-hexane). ^1H NMR ($CDCl_3$): δ = 8.90 (br., 1 H, NH), 8.24 (s, 1 H, N=C*H*N), 7.04–7.37 (m, 10 H, Ar) ppm. ^{13}C NMR ($CDCl_3$): δ = 149.5 (N=*C*HN), 145.2, 129.3, 123.3, 119.1 ppm. IR (KBr): $\tilde{\nu}$ = 3050 (br.), 3052 (w), 2923 (w), 1679 (s), 1660 (s), 1601 (w), 1583 (s), 1488 (s), 1450 (w), 1321 (m), 1209 (m), 1171 (w), 987 (w), 900 (w), 766 (m), 754 (m), 695 (m) cm^{-1}. ESI-MS: *m*/*z* (%) = 197 (100) [M^+]. HRMS: calcd. for $C_{13}H_{12}N_2$+H: 197.10733; found 197.10687. UV/Vis (CH_3CN, 25 °C) λ = 281.5 nm.

***N,N′*-Bis(4-fluorophenyl)formamidine (2b):**[8,22–25] Yield 63% (3.7 g); m.p. 142–144 °C (crystallized from *n*-hexane). ^1H NMR ($CDCl_3$): δ = 9.65 (br., 1 H, NH), 8.07 (s, 1 H, N=C*H*N), 6.97–7.10 (m, 8 H, Ar) ppm. ^{13}C NMR ($CDCl_3$): δ = 161.8, 157.0, 150.2 (N=*C*HN), 141.2, 120.5, 120.4, 116.2, 115.8 ppm. ^{19}F NMR ($CDCl_3$): δ = –120.0 (m) ppm. IR (KBr): $\tilde{\nu}$ = 3428 (w), 2928 (w), 2862 (w), 1671 (s), 1603 (w), 1502 (s), 1380 (m), 1313 (m), 1202 (m), 999 (w), 825 (m), 750 (w), 501 (w) cm^{-1}. ESI-MS: *m*/*z* (%) = 236 (100), 233 (13) [M^+], 227 (41), 214 (24), 159 (23), 149 (48), 133 (26). HRMS: calcd. for $C_{13}H_{10}F_2N_2$+H: 233.08848; found 233.08671. UV/Vis (CH_3CN, 25 °C) λ = 279.5 nm.

***N,N′*-Bis(3,5-difluorophenyl)formamidine (2c):** Yield 51% (3.4 g); m.p. 182 °C. ^1H NMR ($CDCl_3$): δ = 8.03 (s, 1 H, N=C*H*N), 6.46–6.73 (m, 6 H, Ar) ppm. ^{13}C NMR ($CDCl_3$): δ = 165.6, 165.5, 163.2, 163.1, 149.1, 118.3, 103.4, 99.2, 98.9, 98.7 ppm. ^{19}F NMR ($CDCl_3$): δ = –108.6 (m) ppm. IR (KBr): $\tilde{\nu}$ = 3095 (m), 1676 (s), 1614 (s), 1513 (m), 1478 (m), 1453 (m), 1380 (m), 1356 (m), 1322 (m), 1284 (m), 1224 (m), 1161 (m), 1135 (s), 1121 (s), 1034 (m), 986 (s), 869 (m), 855 (m), 838 (m), 788 (w), 748 (w), 676 (m), 649 (w), 594 (w), 565 (w), 531 (w), 510 (w) cm^{-1}. ESI-MS: *m*/*z* (%) = 269 (100) [M^+]. HRMS: calcd. for $C_{13}H_8F_4N_2$+H: 269.06964; found 269.04294. UV/Vis (CH_3CN, 25 °C) λ = 294.5 nm.

***N,N′*-Bis(2,6-difluorophenyl)formamidine (2d):** Yield 89% (5.9 g); m.p. 151 °C (crystallized from *n*-hexane). ^1H NMR ($CDCl_3$): δ = 8.44 (br., 1 H, NH), 7.94 (s, 1 H, N=C*H*N), 6.85–7.10 (m, 6 H, Ar) ppm. ^{13}C NMR ($CDCl_3$): δ = 157.7, 157.6, 154.44, 154.39, 152.8, 152.7, 123.4, 123.2, 123.0, 121.9, 112.0, 111.9, 111.7, 111.6 ppm. ^{19}F NMR ($CDCl_3$): δ = –123.9 (s) ppm. IR (KBr): $\tilde{\nu}$ = 2884 (w), 1669 (s), 1613 (w), 1492 (m), 1466 (m), 1313 (m), 1270 (m), 1240 (w), 1206 (m), 993 (m), 777 (m), 738 (w), 711 (w) cm^{-1}. ESI-MS: *m*/*z* (%) = 269 (100) [M^+]. HRMS: calcd. for $C_{13}H_8F_4N_2$+H: 269.06964; found 269.05377. UV/Vis (CH_3CN, 25 °C) λ = 268.0 nm.

***N,N*-Bis(2,3,5-trifluorophenyl)formamidine (2e):** Yield 71% (5.4 g), m.p. 124 °C (crystallized from *n*-hexane). ^1H NMR ($CDCl_3$): δ = 8.14 (s, 1 H, N=C*H*N), 6.73–6.60 (m, 4 H, Ar) ppm. ^{13}C NMR ($CDCl_3$): δ = 159.4, 156.9, 152.3, 149.8, 149.1, 103.4, 100.4 ppm. ^{19}F NMR ($CDCl_3$): δ = –114.1, –133.3, –159.4 ppm. IR (KBr): $\tilde{\nu}$ = 2974 (w), 1672 (s), 1609 (s), 1514 (m), 1492 (w), 1417 (w), 1315 (s), 1213 (m), 1156 (m), 1107 (s), 1069 (s), 988 (w), 848 (w), 832 (m), 777 (w), 731 (w), 673 (w), 643 (m), 619 (w), 591 (w), 553 (w), 510 (w) cm^{-1}. ESI-MS: *m*/*z* (%) = 305 (100) [M^+], 236 (40), 146 (39). HRMS: calcd. for $C_{13}H_6F_6N_2$+H: 305.05079; found 305.04923. UV/Vis (CH_3CN, 25 °C) λ = 292.0 nm.

***N,N*-Bis(3,4,5-trifluorophenyl)formamidine (2f):** Yield 38% (2.9 g), m.p. 142 °C (crystallized from *n*-hexane). ^1H NMR ($CDCl_3$): δ = 7.89 (s, 1 H, N=C*H*N), 6.61–6.92 (m, 4 H, Ar) ppm. ^{13}C NMR (CD_3CN): δ = 161.8, 157.0, 150.2 (N=*C*HN), 141.3, 120.5, 120.4, 116.2, 115.8 ppm. ^{19}F NMR ($CDCl_3$): δ = –132.8 (s), –166.4, –165.9 (m) ppm. IR (KBr): $\tilde{\nu}$ = 3105 (w), 3010 (w), 2917 (w), 1677 (s), 1619 (s), 1519 (s), 1437 (m), 1398 (w), 1380 (m), 1341 (m), 1280 (s),

Table 5. The data collection and the refinement parameters for **2d**–**2g**, *trans*-**3c**, *cis*-**3c** and *cis*-**3f**.

	2d	**2e**	**2f**	**2g**·toluene
Empirical formula	$C_{13}H_8F_4N_2$	$C_{13}H_6F_6N_2$	$C_{13}H_6F_6N_2$	$C_{20}H_{10}F_{10}N_2$
Formula weight [g/mol]	268.21	304.20	304.20	468.30
Temperature [K]	150(2)	150(2)	150(2)	150(2)
Space group	$P2_1/c$	$P2_1/c$	$P\bar{1}$	$P2_1/n$
a [Å]	7.9581(6)	11.3272(6)	6.9917(6)	12.2830(8)
b [Å]	14.2415(9)	25.5824(14)	7.6522(6)	6.8687(6)
c [Å]	10.1617(9)	8.2359(4)	11.4522(7)	22.2265(17)
α [°]	90	90	83.865(6)	90
β [°]	98.700(8)	99.683(5)	84.241(6)	92.510(6)
γ [°]	90	90	84.642(7)	90
Volume [Å^3]	1138.43(15)	2352.6(2)	604.01(8)	1873.4(2)
Z	4	8	2	4
$D_{cald.}$ [g/cm^3]	1.565	1.718	1.673	1.660
$F(000)$	544	1216	304	936
Crystal size [mm^3]	$0.13\times0.09\times0.08$	$0.17\times0.12\times0.11$	$0.16\times0.15\times0.15$	$0.12\times0.11\times0.09$
θ range [°]	3.36 to 24.99	3.44 to 25.00	3.38 to 25.00	3.49 to 25.00°
Index ranges	$-8 \le h \le 9$	$-13 \le h \le 13$	$-7 \le h \le 8$	$-14 \le h \le 14$
	$-16 \le k \le 16$	$-27 \le k \le 30$	$-9 \le k \le 9$	$-8 \le k \le 8$
	$-12 \le l \le 10$	$-6 \le l \le 9$	$-13 \le l \le 13$	$-24 \le l \le 26$
Reflections collected	8285	9331	4159	12802
Independent reflections	1996	4131	2124	3290
R_{int}	0.0360	0.0433	0.0231	0.0254
Completeness to θ = 25.00° [%]	99.8	99.8	99.8	99.8
Rel. transmission factors	0.9889 and 0.9847	0.9815 and 0.9716	1.000 and 0.9912	0.9850 and 0.9800
Parameters	172	399	194	290
GOF	0.949	0.876	0.933	1.118
Final R indices [$I>2\sigma(I)$][a,b]	R_1 = 0.0343	R_1 = 0.0470	R_1 = 0.0343	R_1 = 0.0464
	wR_2 = 0.0757	wR_2 = 0.0783	wR_2 = 0.0685	wR_2 = 0.1083
R indices (all data)[a,b]	R_1 = 0.0539	R_1 = 0.1085	R_1 = 0.0582	R_1 = 0.0613
	wR_2 = 0.0811	wR_2 = 0.0926	wR_2 = 0.0732	wR_2 = 0.1148
	trans-**3c**·toluene	*cis*-**3f**·DCM	*cis*-**3c**·cyclopentane	
Empirical formula	$C_{49}H_{58}F_8Mo_2N_4O_4$	$C_{43}H_{48}Cl_2F_{12}Mo_2N_4O_4$	$C_{47}H_{60}F_8Mo_2N_4O_4$	
Formula weight [g/mol]	1203.01	1175.63	1088.87	
Temperature [K]	150(2)	150(2)	150(2)	
Space group	$P2_1/c$	$P\bar{1}$	CC	
a [Å]	11.1268(2)	10.7695(11)	10.43190(10)	
b [Å]	20.6347(4)	11.0482(13)	42.3604(4)	
c [Å]	13.1366(3)	21.810(2)	23.5800(2)	
α [°]	90	92.493(9)	90	
β [°]	110.784(2)	103.398(9)	102.6260(10)	
γ [°]	90	100.087(9)	90	
Volume [Å^3]	2819.86(10)	2475.8(5)	10168.01(16)	
Z	2	2	8	
$D_{cald.}$ [g/cm^3]	1.417	1.577	1.423	
$F(000)$	1236	1184	4464	
Crystal size [mm^3]	$0.23\times0.20\times0.12$	$0.26\times0.17\times0.07$	$0.18\times0.16\times0.16$	
θ range [°]	3.35 to 25.00	3.31 to 25.00	3.28 to 25.00	
Index ranges	$-13 \le h \le 13$	$-12 \le h \le 11$	$-12 \le h \le 12$	
	$17 \le k \le 24$	$12 \le k \le 13$	$-50 \le k \le 49$	
	$-15 \le l \le 15$	$-25 \le l \le 25$	$-28 \le l \le 23$	
Reflections collected	21034	18573	37855	
Independent reflections	4960	8705	14796	
R_{int}	0.0185	0.0829	0.0205	
Completeness to θ = 25.00° [%]	99.8	99.7	99.7	
Rel. transmission factors	0.9404 and 0.8901	0.9524 and 0.8383	1.00000 and 0.95080	
Parameters	340	616	1197	
GOF	1.063	0.946	1.025	
Final R indices [$I>2\sigma(I)$][a,b]	R_1 = 0.0357	R_1 = 0.0692	R_1 = 0.0307	
	wR_2 = 0.0921	wR_2 = 0.1268	wR_2 = 0.0817	
R indices (all data)[a,b]	R_1 = 0.0398	R_1 = 0.1385	R_1 = 0.0347	
	wR_2 = 0.0941	*wR_2 = 0.1452*	*wR_2 = 0.0830*	

[a] $R_1 = \Sigma||F_o| - |F_c||/\Sigma|F_o|$. [b] $\omega R_2 = \{\Sigma\,[w(F_o^2 - F_c^2)^2]/\Sigma[w(F_o^2)^2]\}^{1/2}$.

1233 (s), 1044 (s), 983 (m), 874 (m), 853 (m), 841 (m), 824 (w), 785 (m), 712 (w), 689 (w), 642 (w), 585 (w) cm^{-1}. ESI-MS: *m/z* (%) = 304 (8) [M$^+$], 288 (23), 236 (100), 226 (49), 220 (21), 214 (24), 159 (21), 149 (30), 117 (35). HRMS: calcd. for $C_{13}H_6F_6N_2$+H:

305.05079; found 305.05016. UV/Vis (CH_3CN, 25 °C) λ = 271.0 nm.

***N*,*N*′-Bis(2,3,4,5,6-pentafluorophenyl)formamidine (2g):** Yield 74% (5.6 g); m.p. 162 °C (crystallized from *n*-hexane). ^{1}H NMR ($CDCl_3$): δ = 8.28 (s, 1 H, N=C*H*N) ppm. ^{19}F NMR ($CDCl_3$): δ = –152.1 (br), –160.8 (br), –162.6 (br) ppm. IR (KBr): $\tilde{\nu}$ = 2861 (w), 1678 (s), 1640 (m), 1514 (s), 1462 (m), 1380 (w), 1322 (m), 1288 (m), 1170 (w), 1035 (m), 978 (s), 783 (w), 607 (w), 564 (w), 493 (w) cm^{-1}. ESI-MS: *m*/*z* (%) = 377 (100) [M$^+$], 236 (21), 219 (27). HRMS: calcd. for $C_{13}H_2F_{10}N_2$+H: 377.01311; found 305.01062. UV/Vis (CH_3CN, 25 °C) λ = 264.5 nm.

***N*,*N*′-Bis(p-trifluoromethylphenyl)formamidine (2h):**[26–31] Yield 59% (4.9 g), m.p. 166 °C. ^{1}H NMR ($CDCl_3$): δ = 8.42 (br. s, 1 H, NH), 8.21 (s, 1 H, N=C*H*N), 7.60 (d, *J* = 17.8 Hz, 4 H, C_6H_2), 7.16 (d, *J* = 16.3 Hz, 4 H, C_6H_2) ppm. ^{13}C NMR ($CDCl_3$): δ = 162.9, 159.0, 126.8, 126.8, 126.7, 126.6, 119.5, 118.9, 118.1, 114.1 ppm. ^{19}F NMR ($CDCl_3$): δ = –61.8 ppm. IR (KBr): $\tilde{\nu}$ = 2975 (m), 1672 (s), 1609 (s), 1514 (m), 1492 (m), 1418 (m), 1315 (s), 1236 (m), 1214 (m), 1180 (m), 1157 (m), 1107 (s), 1069 (s), 1011 (m), 988 (m), 946 (w), 849 (m), 833 (m), 778 (w), 731 (w), 674 (w), 643 (w), 620 (w), 591 (w), 553 (w), 511 (w) cm^{-1}. ESI-MS: *m*/*z* (%) = 333 (100) [M$^+$], 236 (23), 146 (20). HRMS: calcd. for $C_{15}H_{10}F_6N_2$+H: 333.08209; found 333.08174. UV/Vis (CH_3CN, 25 °C) λ = 300.75 nm.

Synthesis of Mo_2(L–H)$_2$(O*t*Bu)$_4$ (3a–3c and 3e–3f) with L = 2a–2c and 2e–2f, respectively: Mo_2(O*t*Bu)$_6$ (200 mg, 0.32 mmol) was dissolved in pentane (10 mL) and cooled to –20 °C. The corresponding formamidine, **2a**–**2f**, (2:1 molar ratio) was dissolved in DCM and added dropwise to the solution whereupon the colour of the solution slowly turned from bright orange to dark red-brown. After the solution was stirred for three hours, the solution was filtered and all of the volatiles where removed in vacuo. The obtained green-brown solid was dissolved in a mixture of toluene/DCM (1:1) and recrystallized at –20 °C. The obtained crystals were thoroughly crushed and dried in vacuo at elevated temperatures in order to completely remove the cocrystallized solvent for the elemental analysis and the NMR spectroscopic measurements.

Mo_2[2a–H]$_2$(O*t*Bu)$_4$ (3a): Compound **2a** (124 mg, 0.64 mmol) afforded **3a** (230 mg, 0.26 mmol) in 82% yield. $C_{42}H_{58}Mo_2N_4O_4$ (874.8): calcd. C 57.66, H 6.68, N 6.40; found C 57.54, H 6.75, N 6.44. ^{1}H NMR ($CDCl_3$): δ = 8.83 (s, 2 H, N =C*H*N), 6.13–6.32 (m, 20 H, Ar), 1.32 (s, 36 H, *t*Bu) ppm. ^{13}C NMR ($CDCl_3$): δ = 169.6, 145.1, 129.4, 124.4, 123.0, 83.0, 33.0 ppm.

Mo_2[2b–H]$_2$(O*t*Bu)$_4$ (3b): Compound **2b** (179 mg, 0.64 mmol) afforded **3b** (176 mg, 0.19 mmol) in 59% yield. $C_{42}H_{54}F_4Mo_2N_4O_4$ (946.8): calcd. C 53.28, H 5.75, N 5.92; found C 52.97, H 5.74, N 6.01. ^{1}H NMR ($CDCl_3$): δ = 8.88 (s, 2 H, N=C*H*N), 6.11–6.32 (m, 16 H, Ar), 1.40 (s, 36 H, *t*Bu) ppm. ^{13}C NMR ($CDCl_3$): δ = 176.3, 162.3, 146.0, 124.2, 116.0, 81.06, 32.2 ppm. ^{19}F NMR ($CDCl_3$): δ = –118.8 (m) ppm.

Mo_2[2c–H]$_2$(O*t*Bu)$_4$ (3c): Compound **2c** (172 mg, 0.64 mmol) afforded **3c** (176 mg, 0.17 mmol) in 53% yield. The obtained single crystals were suitable for single-crystal X-ray diffraction measurements. $C_{42}H_{50}F_8Mo_2N_4O_4$ (1018.7): calcd. C 49.52, H 4.95, N 5.50; found C 49.93, H 5.01, N 5.71. ^{1}H NMR ($CDCl_3$): δ = 8.97 (s, 2 H, N=C*H*N), 6.00–6.28 (m, 12 H, Ar), 1.43 (s, 36 H, *t*Bu) ppm. ^{13}C NMR ($CDCl_3$): δ = 176.0, 164.2, 150.2, 107.2, 100.1, 82.4, 32.1 ppm. ^{19}F NMR ($CDCl_3$): δ = –108.3 (m) ppm.

Mo_2[2e–H]$_2$(O*t*Bu)$_4$ (3e): Compound **2e** (195 mg, 0.64 mmol) afforded **3e** (237 mg, 0.22 mmol) in 69% yield. $C_{42}H_{46}F_{12}Mo_2N_4O_4$ (1090.7): calcd. C 46.25, H 4.25, N 5.14; found C 46.86, H 4.33, N 5.22. ^{1}H NMR ($CDCl_3$): δ = 9.12 (s, 2 H, N=C*H*N), 6.27–6.36 (m, 4 H, Ar), 6.07–6.21 (m, 4 H, Ar), 1.44 (s, 36 H, *t*Bu) ppm. ^{13}C NMR ($CDCl_3$): δ = 179.1, 158.4, 155.9, 152.1, 149.1, 106.0, 99.5, 80.9, 32.8 ppm. ^{19}F NMR ($CDCl_3$): δ = –114.5 (m), –132.0 (m), –156.2 (m) ppm.

Mo_2[2f–H]$_2$(O*t*Bu)$_4$ (3f): Compound **2f** (193 mg, 0.64 mmol) afforded **3f** (248 mg, 0.23 mmol) in 72% yield. The obtained single crystals were suitable for single-crystal X-ray diffraction measurements. $C_{42}H_{46}F_{12}Mo_2N_4O_4$ (1090.7): calcd. C 46.25, H 4.25, N 5.14; found C 46.11, H 4.20, N 5.32. ^{1}H NMR ($CDCl_3$): δ = 8.87 (s, 2 H, N=C*H*N), 6.13–6.29 (m, 8 H, Ar), 1.46 (s, 36 H, *t*Bu) ppm. ^{13}C NMR ($CDCl_3$): δ = 175.9, 169.9, 152.6, 144.7, 107.5, 82.4, 32.3 ppm. ^{19}F NMR ($CDCl_3$): δ = –132.0 (m), –163.9 (m) ppm.

Supporting Information (see footnote on the first page of this article): The information on the H···F interactions for compounds **2** and the details of the DFT calculations.

Acknowledgments

Financial support by the Technical University of Berlin (Cluster of Excellence, *Unifying Concepts in Catalysis*, EXC 314/1; www.unicat.tu-berlin.de), funded by the Deutsche Forschungsgemeinschaft (DFG) is gratefully acknowledged. S. K. thanks the Fonds der Chemischen Industrie for a Kekulé scholarship and the Berlin International Graduate School of Natural Sciences and Engineering (BIG-NSE) for ideational support. S. I. thanks the Japan Society for the Promotion of Science (JSPS) for financial support of his work.

[1] K. Reichenbächer, H. I. Süss, J. Hulliger, *Chem. Soc. Rev.* **2005**, *34*, 22–30.
[2] "Fluorine in the Life Science Industry", P. Maienfisch (Ed.), *Chimia* **2004**, *58*, 92–162.
[3] G. W. Coates, A. R. Dunn, L. M. Hennling, J. W. Ziller, E. B. Lobkosky, R. H. Grubbs, *J. Am. Chem. Soc.* **1998**, *120*, 3641–3649.
[4] H. Takemura, N. Kon, M. Kotoku, S. Nakashima, K. Otsuka, M. Yasutake, T. Shinmyozu, T. Inazu, *J. Org. Chem.* **2001**, *66*, 2778–2783.
[5] H. Plenio, R. Diodone, *Chem. Ber.* **1996**, *129*, 1211–1217.
[6] R. Uson, J. Fornies, M. Tomas, J. M. Casas, F. A. Cotton, L. R. Falvello, R. Llusar, *Organometallics* **1988**, *7*, 2279–2285.
[7] H. W. Roesky, I. Haiduc, *J. Chem. Soc., Dalton Trans.* **1999**, 2249–2264.
[8] F. A. Cotton, C. A. Murillo, I. Pascual, *Inorg. Chem.* **1999**, *38*, 2182–2187.
[9] F. A. Cotton, T. Ren, *J. Am. Chem. Soc.* **1992**, *114*, 2237–2242.
[10] K. L. Fujdala, T. D. Tilley, *Chem. Mater.* **2004**, *16*, 1035–1047.
[11] J.-G. Ma, Y. Aksu, L. J. Gregoriades, J. Sauer, M. Driess, *Dalton Trans.* **2010**, *39*, 103–106.
[12] S. Krackl, J.-G. Ma, Y. Aksu, M. Driess, *Eur. J. Inorg. Chem.* **2011**, DOI: 10.1002/ejic.201001236.
[13] F. A. Cotton, C. A. Murillo, R. A. Walton, *Multiple Bonds between Metal Atoms*, 3rd ed., Springer Science and Business Media, Inc., New York City, **2005**.
[14] H. Komber, H.-H. Limbach, F. Böhme, C. Kunert, *J. Am. Chem. Soc.* **2002**, *124*, 11955–11963.
[15] T. M. Gilbert, C. B. Bauer, A. H. Bond, R. D. Rogers, *Polyhedron* **1999**, *18*, 1293–1301.
[16] T. M. Gilbert, A. M. Landes, R. D. Rogers, *Inorg. Chem.* **1992**, *31*, 3438–3444.
[17] S. Krackl, A. Company, S. Enthaler, M. Driess, *ChemCatChem* **2011**, DOI: 10.1002/cctc.201100007.
[18] T. A. Budzichowski, M. H. Chisholm, *Polyhedron* **1994**, *13*, 2035–2042.
[19] G. M. Sheldrick, *SHELXL-97*, University of Göttingen, Germany, **1997**.

[20] K. Hirano, S. Urban, C. Wang, F. Glorius, *Org. Lett.* **2009**, *11*, 1019–1022.
[21] W. Eul, G. Gattow, *Z. Anorg. Allg. Chem.* **1986**, *535*, 148–158.
[22] R. Anulewicz, I. Wawer, T. M. Krygowski, F. Männle, H.-H. Limbach, *J. Am. Chem. Soc.* **1997**, *119*, 12223–12230.
[23] L. Meschede, H. H. Limbach, *J. Phys. Chem.* **1991**, *95*, 10267–10280.
[24] H. H. Limbach, L. Meschede, G. Scherer, *Z. Naturforschung, Teil A* **1989**, *44*, 459–472.
[25] R. Rossi, A. Duatti, L. Magon, L. Toniolo, *Inorg. Chim. Acta* **1981**, *48*, 243–246.
[26] T. Ren, C. Lin, E. J. Valente, J. D. Zubkowski, *Inorg. Chim. Acta* **2000**, *297*, 283–290.
[27] S. J. Archibald, N. W. Alcock, D. H. Busch, D. R. Whitcomb, *Inorg. Chem.* **1999**, *38*, 5571–5578.
[28] K. M. Carlson-Day, J. L. Eglin, L. T. Smith, C. Lin, R. J. Staples, D. O. Wipf, *Polyhedron* **1999**, *18*, 817–824.
[29] J. L. Eglin, C. Lin, T. Ren, L. Smith, R. J. Staples, D. O. Wipf, *Eur. J. Inorg. Chem.* **1999**, 2095–2103.
[30] C. Lin, J. D. Protasiewicz, T. Ren, *Inorg. Chem.* **1996**, *35*, 7455–7458.
[31] C. Lin, J. D. Protasiewicz, E. T. Smith, T. Ren, *Inorg. Chem.* **1996**, *35*, 6422–6428.

Received: December 27, 2010
Published Online: March 16, 2011

